Classical and quantum quasi-1D Heisenberg model with competing interactions

1989 J. Phys.: Condens. Matter 1 7941

(http://iopscience.iop.org/0953-8984/1/42/015)

J. Phys.: Condens. Matter **1** (1989) 7941–7950. Printed in the UK

Classical and quantum quasi-1D Heisenberg model with competing interactions

A Pimpinelli, E Rastelli and A Tassi
Dipartimento di Fisica dell'Università, 43100 Parma, Italy

Received 30 March 1989

Abstract. In this paper we examine the zero-temperature phase diagram and ground-state configurations of a Heisenberg Hamiltonian with exchange competition up to third-nearest neighbour in 1D (linear chain). In the classical limit $S \to \infty$ we find that the ground state is ferromagnetic, antiferromagnetic or modulated depending on the interactions. Transitions between the various phases are all first order with the exception of a finite portion of the boundary between the ferromagnetic and the helical phases, where the transition is continuous. We also study the quantum model by means of a perturbative approach that evaluates the zero-point-motion energy to order $1/S$ in the non-collinear phases, thus establishing the relative location of the quantum ground-state configurations. However, one can evaluate to *all orders* in $1/S$ the exact expression of the zero-point motion for vanishing helix wavevectors in the vicinity of the second-order ferro–helix classical transition line. The result is that a finite part of the ferro–helix classical line is swept away by quantum fluctuations and replaced by a first-order transition. The scenario should be realistic at low but finite temperature, and should indicate the relevance of quantum effects even on the critical behaviour in quasi-1D systems with very-low-temperature transitions.

1. Introduction

Modulated structures in spin systems are still subjects of intensive research even after nearly 30 years of experimental and theoretical studies. Such structures can be successfully modelled by means of Heisenberg Hamiltonians with competing interactions, since it is known [1] that exchange competition leads to helical phases in magnetic systems.

The treatment of quantum contributions to the ground-state and excitation energy is still an open problem; recently [2] an approach has been worked out that is an alternative to the usual evaluation of the zero-point-motion energy to leading order in $1/S$. This approach is feasible on the parts of the ferro–helix boundary line where the transition is continuous, and it allows an exact (i.e. to all orders in $1/S$) determination of the region where the ferromagnetic ground state becomes unstable with respect to long-wavelength quantum fluctuations, thus giving way to a first-order transition to a non-collinear phase.

In this work we apply both treatments to the ground states of a third-nearest-neighbour Heisenberg (TNNH) model in 1D (linear chain). A word of caution is needed here. Since both methods rely on spin waves, one could question their employment on a 1D quantum spin model. In fact this model has to be looked at as the limit of a 3D arrangement of chains interacting *via* a weak exchange coupling J', which

0953-8984/89/427941+10$02.50

assures LRO; this coupling is not essential since on the ferro–helix transition line the quantities we compute are not divergent in 1D. Thus the result we obtain can be viewed as providing an upper limit to the quantum effect in the 3D model, with the advantage that every calculation is analytical and hence completely under control. With the same attitude, previous results have been published [3], concerning the same model but with interactions only up to next-nearest neighbour. In that work an open question was left: while for $S > \frac{1}{2}$ the conclusion could be drawn that the transition remains continuous, for $S = \frac{1}{2}$ we could reach no definite answer. The answer to this question is given in this paper.

The plan of the paper is as follows. In §2 we discuss the classical ground state and the zero-temperature phase diagram. It is shown to be partitioned in three regions, with ferro, antiferro and helical ordering respectively. An unusual feature is the appearance of a first-order transition line between the ferro and helical phases. This is not seen on either the triangular or the square lattices with just third-nearest-neighbour interactions [4] (a first-order transition may occur there introducing fourth-nearest-neighbour couplings [5]). The first-order boundary joins a second-order ferro–helix line in a tricritical point. Section 3 is devoted to the evaluation of quantum corrections to the ground-state energy on the second-order ferro–helix boundary. It is seen that for any S-value the tricritical point moves along this boundary in such a way as to reduce the extension of the continuous transition line. In §4 the zero-point-motion energy is computed to leading $1/S$ order in the modulated and antiferromagnetic phases. The respective values are then compared and the boundaries in the quantum ground state are determined. Section 5 contains remarks and conclusions.

2. Classical ground state

The Hamiltonian of our model reads

$$H = -\sum_{\alpha} J_{\alpha} \sum_{i,\delta_{\alpha}} \boldsymbol{S}_i \cdot \boldsymbol{S}_{i+\delta_{\alpha}} - J' \sum_{i,\delta'} \boldsymbol{S}_i \cdot \boldsymbol{S}_{i+\delta'} \tag{1}$$

where δ_{α} and δ' are vectors joining site i with its αth neighbours and with its NN in the adjacent chains, respectively. Here the NN intrachain J_1 and the interchain J' exchange couplings are positive, while the next-nearest-neighbour (NNN) J_2 and the third-nearest-neighbour (TNN) J_3 couplings can have either sign. If J_2 and/or J_3 are negative, the competition between exchange interactions can lead to helical states. On the other hand, there is no competition due to J'; the spins in each chain have identical orientations. In order to obtain the classical ground state we let the Hamiltonian depend on a variational parameter $\boldsymbol{Q}$ by introducing a locally rotated reference frame, then transform from spin operators to Bose operators *via* a Dyson–Maleev transformation [6]. We obtain a bosonic Hamiltonian including terms with up to six operators [7]. Here we write just a few terms, the only ones that matter in our computations. We take $J' = 0$ and the lattice constant equal to 1

$$H = E_0(\boldsymbol{Q}) + \sum_k A_k a_k^{\dagger} a_k + \frac{1}{2} \sum_k B_k (a_k^{\dagger} a_{-k}^{\dagger} + a_k a_{-k}) + (2NS)^{-1} \sum_{1,2,3,4} V_{1,2,3,4} \delta(1+2,3+4) a_1^{\dagger} a_2^{\dagger} a_3 a_4 \tag{2}$$

where 1 denotes $\boldsymbol{k}_1$, 2 denotes $\boldsymbol{k}_2$, etc and, in the small-Q limit,

$$E_0(\boldsymbol{Q}) = -2J_1NS^2[1 + j_2 + j_3 - \tfrac{1}{2}Q^2(1 + 4j_2 + 9j_3) + \tfrac{1}{24}Q^4(1 + 16j_2 + 81j_3)] \tag{3}$$

with $j_\alpha = J_\alpha/J_1$ $A_{\boldsymbol{k}} = 8J_1S\epsilon_{\boldsymbol{k}}$, where

$$\epsilon_{\boldsymbol{k}} = \frac{1}{2}\sum_{m=1}^{3}\hat{j}_m(1 - \cos k_m). \tag{4}$$

Here

$$\hat{j}_1 = 1 \qquad \hat{j}_2 = j_2 \qquad \hat{j}_3 = j_3 \tag{5}$$

and

$$k_1 = k_z \qquad k_2 = 2k_z \qquad k_3 = 3k_z. \tag{6}$$

Furthermore,

$$B_{\boldsymbol{k}} = -4J_1Sb_{\boldsymbol{k}}Q^2 \tag{7}$$

where

$$b_{\boldsymbol{k}} = \tfrac{1}{4}(\cos k_1 + 4j_2\cos k_2 + 9j_3\cos k_3). \tag{8}$$

$V_{1,2,3,4}$ is the well known Dyson–Maleev [6] interaction potential, that we need only [2] for $Q = 0$ and $\boldsymbol{k}_1 = -\boldsymbol{k}_2 \equiv \boldsymbol{k}$ and $\boldsymbol{k}_3 = -\boldsymbol{k}_4 \equiv \boldsymbol{q}$,

$$V_{\boldsymbol{k},\boldsymbol{q}} = -4J_1S\sum_{m=1}^{3}\hat{j}_m(1 - \cos k_m)(1 - \cos q_m). \tag{9}$$

Minimising $E_0(\boldsymbol{Q})$ we find the zero-temperature phase diagram shown in figure 1. In region F spins are arranged ferromagnetically, that is $\boldsymbol{Q} = (0, 0, 0)$. Region AF supports an intrachain antiferromagnetic ordering, with $\boldsymbol{Q} = (0, 0, \pi)$. Finally, in region H we find a modulated structure characterised by a wavevector $\boldsymbol{Q} = (0, 0, Q)$ where

$$\cos Q = \frac{-j_2 - [j_2^2 - 3j_3(1 - 3j_3)]^{1/2}}{6j_3} \tag{10a}$$

It is apparent that

$$\cos Q = \frac{-j_2 + [j_2^2 - 3j_3(1 - 3j_3)]^{1/2}}{6j_3} \tag{10b}$$

is another extremum for the classical energy, but it is seen to be always a maximum in the helical phase.

The boundaries between the various phases are given by

(i) I–II

$$j_3 = -1 \tag{11a}$$

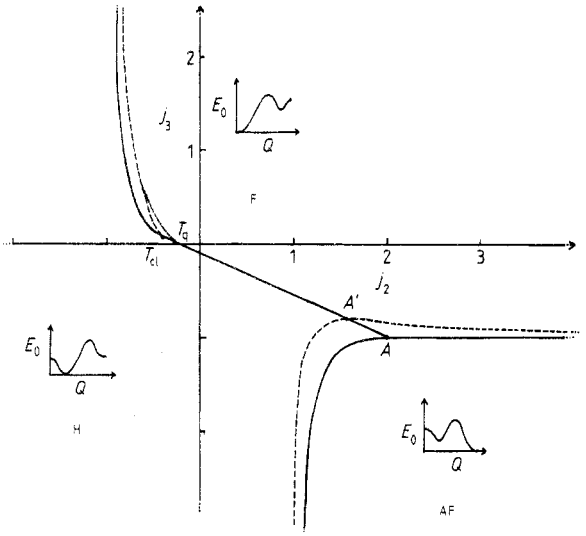

Figure 1. Zero-temperature phase diagram of the 1D-TNN Heisenberg model. Full curves are the classical ($S \to \infty$) phase boundaries, T_{cl} being the classical tricritical point. T_{cl}–A is the second-order ferro–helix phase transition line. All other transitions are first order. A qualitative sketch of $E_0(Q)$ is given for ferromagnetic (F), helix (H), antiferromagnetic (AF) configurations. Broken curves are obtained by a first-order calculation in $1/S$. The dotted curve is conjectured. T_q is the tricritical point obtained by a T-matrix calculation. The only second-order phase transition surviving quantum fluctuations is the portion T_q–A' of the F–H transition line. Quantum corrections shown in this figure refer to $S = 1$.

(ii) I–III

$$j_3 = -\tfrac{1}{9}(1 + 4j_2) \qquad \text{if } -\tfrac{2}{5} < j_2 < 2 \tag{11b}$$

$$j_3 = \frac{j_2^2}{4(1 + j_2)} \qquad \text{if } j_2 < -\tfrac{2}{5} \tag{11c}$$

(iii) II–III

$$j_3 = \frac{j_2^2}{4(1 - j_2)}. \tag{11d}$$

The F–H transition is continuous along the curve (11*b*), while it is first order along the curve (11*c*) where Q jumps discontinuously from zero to a value such that $\cos Q = -(2+3j_2)/2j_2$. Curves (11*b*) and (11*c*) meet at the *classical* tricritical point $T_{cl} = (-\frac{2}{5}, \frac{1}{15})$. On the line $j_3 = \frac{1}{3}$ for $j_2 < -\frac{2}{3}$, one has $Q = \frac{1}{2}\pi$ independently of j_2. All other transitions are first order. On the line (11*d*) one has $\cos Q = -(2 - 3j_2)/2j_2$. A is a triple point where the three phases coexist.

Notice that the equation of the line A–T_{cl} is nothing other than the condition for the coefficient of Q^2 in equation (3) to vanish; and in fact this is just what is needed for a continuous transition to occur, together with the requirement that the coefficient of Q^4 be positive. At the tricritical point T_{cl} both the coefficient of Q^2 and that of Q^4 vanish, while Q^6 has a positive coefficient, so that the transition starts being discontinuous where the coefficient of Q^4 becomes negative. We stress that this is a very simple model in which a first-order ferro–helix transition and a tricritical point are present at $T = 0$,

as a result of the competition of interactions; this is not limited to 1D, since it is clear that interchain exchange has no bearing on ground-state configurations. The study of this classical model at finite temperature should prove quite interesting.

3. Quantum corrections to ground-state energy: T-matrix calculation

As we said before, the vanishing of e_2, the coefficient of Q^2 in equation (3), is a necessary but not sufficient condition for the continuity of the ferro–helix transition; one must require that the coefficient of the following term, e_4, be positive. Now, it has been proved possible [2] to compute exactly the contribution of the Hamiltonian (2) to these two coefficients and thus to establish their sign. It turns out that e_2 has no quantum contribution, while e_4 is given by [2]

$$e_4 = -J_1 N S^2 \frac{1}{12}(1 + 16j_2 + 81j_3) - 4J_1 NS\left(I_0 + \frac{1}{2S}\sum_{m,n=1}^{3} \hat{j}_m (A^{-1})_{mn} I_m I_n\right) \tag{12}$$

where I_0, I_m, I_n are integrals explicitly given in the Appendix and A is the matrix

$$A_{mn} = \delta_{mn} - (1/2S)\hat{j}_n D_{mn}. \tag{13}$$

D_{mn} are also integrals given in the Appendix. All integrals are convergent if computed on the line $1 + 4j_2 + 9j_3 = 0$ with $-\frac{2}{5} < j_2 < 2$ and all integrations can be performed analytically in 1D. It is clear from equation (12) that e_4 may change sign in this interval and indeed it does. In table 1 we show the values of j_2 and j_3 at which $e_4 = 0$ for various S. T_q is the *quantum* tricritical point, that is the classical tricritical point T_{cl} shifted by quantum effects. As one could expect, the quantum effect increases as the value of S decreases.

Table 1. Values of j_2 and j_3 for which $e_4 = 0$ (T_q) on the F-H phase boundary for selected values of S.

S	j_2	j_3
1/2	−0.25	0
1	−0.325	0.033
3/2	−0.342	0.041
2	−0.351	0.045
5/2	−0.358	0.048
∞	−0.4	1/15

We also expect that interchain coupling reduces the extent of the first-order region, since it reduces quantum fluctuations, in agreement with what is found in other 2D and 3D models [7, 8]. It can be seen that for $S = \frac{1}{2}$, T_q occurs at $j_3 = 0$. This is the reason why we were not able to establish the order of the transition when we considered only NNN interactions [3]; by chance we had just obtained the tricritical point in the model with third-nearest-neighbour interactions. This finding is consistent with the result by Hamada *et al* [9] who established that the exact ground state is ferromagnetic (degenerate with a resonating valence bond (RVB) state) for $S = \frac{1}{2}$ and $j_2 = -\frac{1}{4}$. Since from our computation the instability of the ferromagnetic ground state against magnon–magnon interaction, in the presence of competing exchange, is apparent, an interesting question arises concerning the stability of the RVB state against the introduction of further neighbour exchange couplings.

4. Zero-point-motion energy in non-collinear phases

In this section we report the evaluation of the *quantum* zero-temperature phase diagram. To this end we go back to the Hamiltonian (2) and we compute its ground state for *arbitrary* Q, including the first correction in the $1/S$ expansion. This gives

$$E_G(\boldsymbol{Q}) = E_0(\boldsymbol{Q})\left(1+\frac{1}{S}\right)+\frac{1}{2}\sum_k E_k \tag{14}$$

where E_k is the spin-wave energy spectrum

$$E_k = \sqrt{S_k D_k} \tag{15}$$

and

$$S_k = 2J_1 S\sum_\alpha \sum_{\delta_\alpha} j_\alpha(\cos \boldsymbol{Q}\cdot\boldsymbol{\delta}_\alpha - \cos \boldsymbol{k}\cdot\boldsymbol{\delta}_\alpha) \tag{16}$$

$$D_k = 2J_1 S\sum_\alpha \sum_{\delta_\alpha} j_\alpha \cos \boldsymbol{Q}\cdot\boldsymbol{\delta}_\alpha(1-\cos \boldsymbol{k}\cdot\boldsymbol{\delta}_\alpha). \tag{17}$$

Since E_k is real only for $\boldsymbol{Q}=\boldsymbol{Q}_c$, where $\boldsymbol{Q}_c$ is the helix wavevector which minimises the *classical* ground-state energy, we computed E_G fixing the spin-wave spectrum on the classical boundary and letting E_0 vary. This is correct at the leading order in $1/S$ since the shift of the classical phase boundary is expected to be of order $1/S$, so that we may use the classical quantities in the zero-point-motion energy, whose leading order is $1/S$. The comparison between the energies of the H, AF, F phases is performed by extrapolating the zero-point-motion energy evaluated on the corresponding classical phase boundaries (see equations (11)). The extrapolation is performed ascribing the zero-point-motion energy of a point of the classical phase boundary to all points of the parameter space lying on straight lines perpendicular to the classical phase boundary within a region of size $1/S$. The classical energies of different configurations are expanded as functions of $1/S$ starting from their common value on their classical phase boundary, to be consistent with the treatment of the zero-point motion described above.

We now consider the neighbourhood of the F–H transition line described by

$$j_3 = \frac{x^2}{4(x+1)}+\frac{a}{S} \tag{18}$$

$$j_2 = x+\frac{b}{S} \tag{19}$$

$$ax(2+x)+4b(x+1)^2 = 0 \tag{20}$$

where $-1 < x < -\frac{2}{5}$. From the condition

$$E_G^H = E_G^F \tag{21}$$

we obtain the shift of the H–F transition line.

$$a = \frac{8x^3(x+1)^2}{(5x+2)[16(x+1)^4+x^2(x+2)^2]}\left(\frac{x^2+4(x+1)^2}{4(x+1)}-\delta_H\right) \tag{22}$$

$$b = \frac{2x^4(x+2)}{(5x+2)[16(x+1)^4+x^2(x+2)^2]}\left(\frac{x^2+4(x+1)^2}{4(x+1)}-\delta_H\right) \tag{23}$$

where

$$\delta_H = \frac{1}{\pi}\int_0^\pi dk \left|\frac{x}{x+1}\left(\cos k + \frac{3x+2}{2x}\right)\right| (1-\cos k)\left(\frac{19x^3+46x^2+36x+8}{4x}\right.$$
$$\left. -(2x+1)(2+x)\cos k - \frac{(3x+2)(3x^2+6x+2)}{x}\cos^2 k\right)^{1/2}. \tag{24}$$

Notice that the present approach does not suggest any shift of T_{cl}. This is a clear limitation of the $1/S$ approximation, since the exact T-matrix calculation shows that T_{cl} is replaced by T_q. For this reason we interpolate between the $1/S$ and the T-matrix result in the neighbourhood of T_{cl} as is shown in figure 1, where the phase diagram for $S = 1$ is given.

Consider now the neighbourhood of the H–AF transition line given by

$$j_3 = -\frac{x^2}{4(x-1)} + \frac{a}{S} \tag{25}$$

$$j_2 = x + \frac{b}{S} \tag{26}$$

$$ax(2-x) + 4b(x-1)^2 = 0 \tag{27}$$

where $1 < x < 2$. From the condition

$$E_G^H = E_G^{AF} \tag{28}$$

we have

$$a = \frac{8x^3(x-1)^2}{(5x-2)[16(x-1)^4 + x^2(2-x)^2]}(\delta_H - \delta_{AF}) \tag{29}$$

$$b = -\frac{2x^4(2-x)}{(5x-2)[16(x-1)^4 + x^2(2-x)^2]}(\delta_H - \delta_{AF}) \tag{30}$$

where

$$\delta_H = \frac{1}{\pi}\int_0^\pi dk\, \frac{x}{x-1}\sin k \left|\cos k - \frac{3x-2}{2x}\right| \left(\frac{19x^3-46x^2+36x-8}{4x}\right.$$
$$\left. +(2x-1)(2-x)\cos k - \frac{(3x-2)(3x^2-6x+2)}{x}\cos^2 k\right)^{1/2} \tag{31}$$

$$\delta_{AF} = \frac{1}{\pi}\frac{(3x-2)^2(3x-4)+4x^3}{6x(x-1)}. \tag{32}$$

Finally we give the AF–F transition line. We have to solve the equation

$$E_G^{AF} = E_G^F \tag{33}$$

which leads to the new AF–F boundary

$$j_3 = -1 + \frac{1}{2S}\left(j_2 - \frac{2}{\pi}\int_0^\pi dk\, \sin k\,[(j_2+2\cos^2 k)^2 - (j_2+2)^2\cos^2 k]^{1/2}\right) \tag{34}$$

for $j_2 > 2$. Equation (34) may be expressed in terms of elliptic integral as follows:

$$j_3 = -1 + \frac{j_2}{2S}\left(1 - \frac{4}{3\pi}\left[(j_2^2/4+1)E(2/j_2) - (j_2^2/4-1)K(2/j_2)\right]\right) \tag{35}$$

where

$$E(k) = \int_0^{\pi/2} \mathrm{d}\alpha \sqrt{1 - k^2 \sin^2 \alpha} \tag{36}$$

and

$$K(k) = \int_0^{\pi/2} \frac{\mathrm{d}\alpha}{\sqrt{1 - k^2 \sin^2 \alpha}} \tag{37}$$

are the complete elliptic integrals of the second and first kinds, respectively. For $j_2 \to 2$ equation (35) gives

$$j_3 = -1 + \frac{1}{S}\left(1 - \frac{8}{3\pi}\right) + \frac{1}{2S}(j_2 - 2)\left(1 - \frac{4}{\pi}\right) \tag{38}$$

while for $j_2 \to \infty$ one obtains

$$j_3 = -1 + \frac{1}{4Sj_2}. \tag{39}$$

The quantum scenario shown in figure 1 for $S = 1$ is expected to undergo minor changes in the 3D model of weakly interacting chains. This is an interesting feature of our result because the general expectation is that quantum effects have minor relevance on the critical behaviour. A large part of the renormalisation group studies of critical phenomena are based on a classical evaluation of the Landau–Ginzburg–Wilson free energy: indeed, the observables are treated as commuting quantities in the ϵ-expansion approach (see for instance [10]). In our model we find that quantum effects strongly affect the zero-temperature phase diagram, at least in some regions of the parameter space. This could suggest that a classical treatment of the spin variables in a renormalisation group analysis could neglect interesting features of quantum systems. This point deserves further theoretical investigation.

5. Conclusions

We have found the zero-temperature phase diagram of a classical Heisenberg model in which competing interactions up to third-nearest neighbour along one spatial direction are assumed. The diagram is characterised by two collinear (F and AF) and one modulated phase (H). All phase boundaries are first order except a finite portion of the H–F transition line which is second order. Then we have studied the corresponding quantum phase diagram in the 1D limit employing spin waves. We have computed the energy of the various ground-state configurations to leading order in $1/S$, in order to obtain the phase boundaries with quantum corrections. Finally we have summed to all orders in $1/S$ the perturbative series for the coefficients of Q^2 and Q^4 in the small-Q development of the ground-state energy along the F–H continuous transition line. Such computations allowed us to conclude that long-wavelength quantum fluctuations induced a first-order character in a portion of this line, and the extent of this portion depends on the value of S, being maximal for small S.

Appendix

In this Appendix we give the explicit form of the integrals appearing in equations (12) and (13). The integrals to be computed are

$$I_0 = \frac{1}{N}\sum_k \frac{b_k^2}{4\epsilon_k} \tag{A1}$$

$$I_m = \frac{1}{N}\sum_k \frac{b_k(1-\cos k_m)}{2\epsilon_k} \tag{A2}$$

$$D_{mn} = D_{nm} = \frac{1}{N}\sum_k \frac{(1-\cos k_m)(1-\cos k_n)}{\epsilon_k} \tag{A3}$$

where

$$\epsilon_k = \sum_{m=1}^{3} \hat{\jmath}(1-\cos k_m). \tag{A4}$$

We have

$$I_0 = -\frac{1}{8192 j_3^2}\{5625 j_3^3 + 2331 j_3^2 - 605 j_3 + 25 + [(1-15j_3)/(1+j_3)]^{1/2}(135 j_3^3 - 459 j_3^2 + 405 j_3 - 25)\} \tag{A5}$$

$$I_1 = \frac{1}{64 j_3}\{5 - 27 j_3 - (5-3j_3)[(1-15j_3)/(1+j_3)]^{1/2}\} \tag{A6}$$

$$I_2 = \frac{1}{256 j_3^2}\{117 j_3^2 - 38 j_3 + 5 - (5-3j_3)[(1+j_3)/(1-15j_3)]^{1/2}\} \tag{A7}$$

$$D_{12} = \frac{1}{2j_3}\left[\left(\frac{1+j_3}{1-15j_3}\right)^{1/2} - 1\right] \tag{A8}$$

$$D_{13} = \frac{1}{8 j_3^2}\left(\frac{(1-3j_3)^2}{[(1+j_3)(1-15j_3)]^{1/2}} - 1 - j_3\right) \tag{A9}$$

$$D_{23} = \frac{1}{32 j_3^3}\left[(1-3j_3)^2\left(\frac{1-15j_3}{1+j_3}\right)^{1/2} - 49 j_3^2 - 2j_3 - 1\right]. \tag{A10}$$

From the sum rules

$$I_1 + j_2 I_2 + j_3 I_3 = 0 \tag{A11}$$

$$D_{11} + j_2 D_{12} + j_3 D_{13} = 1 \tag{A12}$$

$$D_{21} + j_2 D_{22} + j_3 D_{23} = 1 \tag{A13}$$

$$D_{31} + j_2 D_{32} + j_3 D_{33} = 1 \tag{A14}$$

with $j_2 = -\frac{1}{4}(1 + 9j_3)$, we get the remaining integrals. The coefficient of the Q^4 term (12) becomes

$$e_4 = 2J_1 NS^2 \left[\frac{1}{8}(1 - 15j_3) - \frac{2}{S}\left(I_0 + \frac{1}{2S}\frac{n}{d}\right)\right] \tag{A15}$$

where

$$n = \left(1 - \frac{1}{2S}\right)\left(I_1^2 + j_2 I_2^2 + \frac{1}{j_3}(I_1 + j_2 I_2)^2\right) + \frac{1}{2S}\frac{1 + j_2 + j_3}{j_3}$$
$$\left[(D_{12} + j_3 D_{23})I_1^2 + 2j_2 D_{12} I_1 I_2 + j_2(j_2 D_{12} + j_3 D_{13})I_2^2\right] \tag{A16}$$

$$d = \left(1 - \frac{1}{2S}\right)^2 + \left(1 - \frac{1}{2S}\right)\frac{1}{2S}\left[(1 + j_2)D_{12} + (1 + j_3)D_{13} + (j_2 + j_3)D_{23}\right]$$
$$+ \left(\frac{1}{2S}\right)^2 (1 + j_2 + j_3)(D_{12}D_{13} + j_2 D_{12}D_{23} + j_3 D_{13}D_{23}). \tag{A17}$$

One can easily see that for $j_3 \to 0$ the previous equations reduce to those of [3], as expected.

References

[1] Villain J 1959 *J. Phys. Chem. Solids* **11** 303
[2] Harris A B and Rastelli E 1988 *J. Appl. Phys.* **63** 3083
[3] Pimpinelli A, Rastelli E and Tassi A 1988 *J. Phys. C: Solid State Phys.* **21** L835
[4] Rastelli E, Tassi A and Reatto L 1979 *Physica* B **97** 1
[5] Harris A B, Rastelli E and Tassi A 1988 *J. Physique* **49** C8 1395
[6] Dyson F J 1956 *Phys. Rev.* **102** 1217
Maleev S V 1958 *Sov. Phys.–JETP* **6** 776
[7] Rastelli E and Harris A B 1989 *Phys. Rev.* B in press
[8] Harris A B, Pimpinelli A, Rastelli E and Tassi A 1989 *J. Phys.: Condens. Matter* **1** 3821
[9] Hamada T, Kane J, Nakagawa S and Natsume Y 1988 *J. Phys. Soc. Japan* **57** 1891
[10] Ma S K 1976 *Modern Theory of Critical Phenomena* (London: Benjamin)